

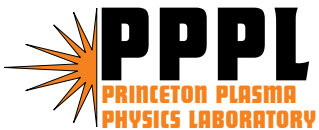
PPPL-4091

PPPL-4091

Status and Plans for the National Spherical Torus Experimental Research Facility

M. Ono, M.G. Bell, R.E. Bell, J.M. Bialek,
T. Bigelow, M. Bitter, et al.

July 2005



PPPL Report Disclaimers

Full Legal Disclaimer

This report was prepared as an account of work sponsored by an agency of the United States Government. Neither the United States Government nor any agency thereof, nor any of their employees, nor any of their contractors, subcontractors or their employees, makes any warranty, express or implied, or assumes any legal liability or responsibility for the accuracy, completeness, or any third party's use or the results of such use of any information, apparatus, product, or process disclosed, or represents that its use would not infringe privately owned rights. Reference herein to any specific commercial product, process, or service by trade name, trademark, manufacturer, or otherwise, does not necessarily constitute or imply its endorsement, recommendation, or favoring by the United States Government or any agency thereof or its contractors or subcontractors. The views and opinions of authors expressed herein do not necessarily state or reflect those of the United States Government or any agency thereof.

Trademark Disclaimer

Reference herein to any specific commercial product, process, or service by trade name, trademark, manufacturer, or otherwise, does not necessarily constitute or imply its endorsement, recommendation, or favoring by the United States Government or any agency thereof or its contractors or subcontractors.

PPPL Report Availability

This report is posted on the U.S. Department of Energy's Princeton Plasma Physics Laboratory Publications and Reports web site in Fiscal Year 2005. The home page for PPPL Reports and Publications is: http://www.pppl.gov/pub_report/

Office of Scientific and Technical Information (OSTI):

Available electronically at: <http://www.osti.gov/bridge>.

Available for a processing fee to U.S. Department of Energy and its contractors, in paper from:

U.S. Department of Energy
Office of Scientific and Technical Information
P.O. Box 62
Oak Ridge, TN 37831-0062
Telephone: (865) 576-8401
Fax: (865) 576-5728
E-mail: reports@adonis.osti.gov

National Technical Information Service (NTIS):

This report is available for sale to the general public from:

U.S. Department of Commerce
National Technical Information Service
5285 Port Royal Road
Springfield, VA 22161
Telephone: (800) 553-6847
Fax: (703) 605-6900
Email: orders@ntis.fedworld.gov
Online ordering: <http://www.ntis.gov/ordering.htm>

Status and plans for the National Spherical Torus Experimental Research Facility*

M. Ono, M.G. Bell, R.E. Bell, J.M. Bialek¹, T. Bigelow², M. Bitter, T.M. Biewer³, W. Blanchard, J. Boedo⁴, C. Bush², J. Chrzanowski, D.S. Darrow, L. Dudek, R. Feder, J.R. Ferron⁵, J. Foley⁶, E.D. Fredrickson, D.A. Gates, G. Gettelfinger, T. Gibney, R. Harvey⁷, R. Hatcher, W. Heidbrink⁸, T.R. Jarboe⁹, D.W. Johnson, M. Kalish, R. Kaita, S.M. Kaye, C. Kessel, S. Kubota¹⁰, H.W. Kugel, G. Labik, B.P. LeBlanc, K. C. Lee¹¹, F.M. Levinton⁶, J. Lowrance¹², R. Maingi², J. Manickam, R. Maqueda⁶, R. Marsala, D. Mastravito, E. Mazzucato, S.S. Medley, J. Menard, D. Mueller, T. Munsat¹³, B.A. Nelson⁹, C. Neumeyer, N. Nishino¹⁴, H.K. Park, S.F. Paul, T. Peebles¹⁰, E. Perry, Y.-K. M. Peng², C.K. Phillips, R. Pinsker⁵, S. Ramakrishnan, R. Raman⁹, P. Roney, A.L. Roquemore, P.M. Ryan², S.A. Sabbagh¹, H. Schneider, C.H. Skinner, D. R. Smith, A.C. Sontag¹, V. Soukhanovskii¹⁵, T. Stevenson, D. Stotler, B.C. Stratton, D. Stutman¹⁶, D.W. Swain², E. Synakowski, Y. Takase¹⁷, G. Taylor, K.L. Tritz¹⁶, A. Von Halle, J. Wilgen², M. Williams, J.R. Wilson, I. Zatz, W. Zhu¹, S.J. Zweben, R. Akers¹⁸, P. Beiersdorfer¹⁵, P.T. Bonoli³, C. Bourdelle¹⁹, M.D. Carter², C. S. Chang²⁰, W. Choe²¹, W. Davis, S.J. Diem, C. Domier¹², R. Ellis, P.C. Efthimion, A. Field¹⁸, M. Finkenthal¹⁶, E. Fredd, G. Y. Fu, A. Glasser²², R.J. Goldston, L.R. Grisham, N. Gorelenkov, L. Guazzotto²³, R. J. Hawryluk, P. Heitzenroeder, K.W. Hill, W. Houlberg², J.C. Hosea, D. Humphreys⁵, C. Jun, J.H. Kim²¹, S. Krasheninnikov⁴, L.L. Lao⁵, S.G. Lee²⁴, J. Lawson, N.C. Luhmann¹², T.K. Mau⁴, M.M. Menon², O. Mitarai²⁵, M. Nagata²⁶, G. Oliaro, D. Pacella²⁷, R. Parsells, A. Pigarov⁴, G.D. Porter¹⁵, A.K. Ram³, D. Rasmussen², M. Redi, G. Rewoldt, J. Robinson, E. Ruskov⁸, J. Schmidt, I. Semenov²⁸, K. Shaing²⁹, K. Shinohara³⁰, M. Schaffer⁵, P. Sichta, X. Tang²², J. Timberlake, M. Wade², W.R. Wampler³¹, Z. Wang²², R. Woolley, G.A. Wurden²², X. Xu¹⁵

¹ Columbia University, New York, N.Y., USA

² Oak Ridge National Laboratory, Oak Ridge, Tennessee, USA

³ Massachusetts Institute of Technology, Cambridge, Massachusetts, USA

⁴ University of California, San Diego, California, USA

⁵ General Atomics, San Diego, California, USA

⁶ Nova Photonics, Princeton, New Jersey, USA

⁷ CompX, Del Mar, California, USA

⁸ University of California, Irvine, California, USA

⁹ University of Washington, Seattle, Washington, USA

¹⁰ University of California, Los Angeles, California, USA

¹¹ University of California, Davis, California, USA

¹² Princeton Scientific Instruments, Princeton, New Jersey, USA

¹³ University of Colorado, Boulder, CO, USA

¹⁴ Hiroshima University, Hiroshima, Japan

¹⁵ Lawrence Livermore National Laboratory, Livermore, California, USA

¹⁶ Johns Hopkins University, Baltimore, Maryland, USA

¹⁷ University of Tokyo, Tokyo, Japan

¹⁸ Euratom-UKAEA Fusion Association, Abingdon, Oxfordshire, United Kingdom

¹⁹ CEA Cadarache, France

²⁰ New York University, NYU, NY, USA

²¹ Korea Advanced Institut of Science and Technology, Taejon, Republic of Korea

²² Los Alamos National Laboratory, Los Alamos, New Mexico, USA

²³ University of Rochester, Rochester, NY, USA

²⁴ Korea Basic Science Institute, Taejon, Republic of Korea

²⁵ Kyushu Tokai University, Kumamoto, Japan

²⁶ Himeji Institute of Technology, Okayama, Japan

²⁷ ENEA, Frascati, Italy

²⁸ Kurcahtov Institute, RUSSIA

²⁹ University of Wisconsin, Wisconsin, USA

³⁰ JAERI, Naka, Japan.

³¹ Sandia National Laboratories, Albuquerque, New Mexico, USA

An overview of the research capabilities and the future plans on the MA-class National Spherical Torus Experiment (NSTX) at Princeton is presented. NSTX research is exploring the scientific benefits of modifying the field line structure from that in more conventional aspect ratio devices, such as the tokamak. The relevant scientific issues pursued on NSTX include energy confinement, MHD stability at high β , non-inductive sustainment, solenoid-free start-up, and power and particle handling. In support of the NSTX research goal, research tools are being developed by the NSTX team. In the context of the fusion energy development path being formulated in the US, an ST-based Component Test Facility (CTF) and, ultimately a high β Demo device based on the ST, are being considered. For these, it is essential to develop high performance (high β and high confinement), steady-state (non-inductively driven) ST operational scenarios and an efficient solenoid-free start-up concept. We will also briefly describe the Next-Step-ST (NSST) device being designed to address these issues in fusion-relevant plasma conditions.

* This research was supported by DoE contract DE-AC02-76CH03073

Keywords : Magnetic Fusion, NSTX, Spherical Torus

1. INTRODUCTION

The spherical-torus (ST)⁽¹⁾ research conducted worldwide has made remarkable progress in recent years. The National Spherical Torus Experiment (NSTX)^(2,3) at the Princeton Plasma Physics Laboratory (PPPL) is a proof-of-principle facility built to carry out research on this plasma configuration. The NSTX team is presently focusing on two broad scientific goals relevant to fusion research in general and the ST in particular. First as a major fusion research facility for the US Fusion Energy Science, an important near term goal for NSTX is to utilize the rich and diverse ST plasma properties in NSTX to develop a deeper understanding of critical high-temperature toroidal plasma physics issues for fusion; this research will contribute to the space-astrophysical plasma sciences as well.⁽⁴⁾ Secondly, an important longer term goal of NSTX is to assess the attractiveness of the ST as a fusion energy concept such as an ST-based



Fig. 1. An aerial view of the NSTX Test Cell. The NSTX device is in the center. The NBI beam box is located in the far side and the HHFW transmission lines to the right..

Component Test Facility (CTF) and a "Demo" plant. Accordingly, the NSTX research plan aims to develop high performance (*i.e.* high- β and high confinement), steady-state (non-inductively-driven) ST operational scenarios and efficient solenoid-free start-up concepts.^(5,6) The research results obtained should also be applicable to other concepts and configurations, including existing tokamaks and future burning plasma experiments, such as ITER and NSST(Next-Step ST). In support of these physics goals, an upgrade plan for the implementation of the necessary research tools has been developed. The research tools available and planned will be discussed in the following sections for key science areas.

2. NSTX FACILITY

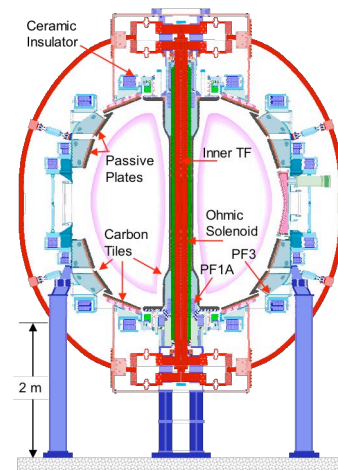


Fig. 2. NSTX Device Cross Section Schematic.

2.1 DEVICE OVERVIEW

NSTX is a major component of the restructured U.S. Fusion Energy Sciences Program, which encompasses both the investigation of innovative confinement concepts and the advancement of the underlying physics to strengthen the scientific basis for attractive fusion power. To accomplish this mission, the NSTX facility, shown in Figs. 1 and 2, presently has the following capabilities:

- Low aspect ratio, $R/a \geq 1.26$, and strongly shaped plasma cross-section with nominal elongation $\kappa \leq 2.7$ and triangularity $\delta \leq 0.8$;
- Plasma current I_p up to 1.4 MA which exceeds the total toroidal magnet current;
- Coaxial Helicity Injection (CHI) for Solenoid-free startup to 0.4 MA;
- High Harmonic Fast Wave system (6 MW), Neutral Beam Injection (7 MW) and CHI for heating, current drive, and current profile control;
- Close-fitting conducting plates to access high plasma β ;
- Error Field and Resistive Wall Mode Feed-back coils to stabilize MHD modes occurring at high plasma beta; and
- Toroidal field pulse length (at 0.3 T) up to 3 s which exceeds the plasma skin time (~ 0.3 s) to test the physics of steady-state operation.

The NSTX facility has already achieved or exceeded many of its original design capabilities⁽⁷⁻⁸⁾ In particular, the plasma current, a key parameter for plasma performance, reached 1.4 MA, 40 % over the original design value of 1 MA. The highest elongation of 2.7 is also significantly higher than the original target value of ~ 2 . The achieved plasma toroidal beta of $\sim 40\%$ has reached the original target. In the following section, we will describe the status and plans for the basic NSTX device magnets, vacuum, and plasma control systems. We will describe the diagnostic systems in Sec. 3, the research tools in Sec. 4, and the advanced research tools in Sec. 5.

2.2. DEVICE SUBSYSTEMS

Magnet Systems – The NSTX magnet systems are composed of the coils contained in the center-stack assembly (inner TF, OH solenoid, top and bottom PF 1A coils and a bottom PF 1B coil, thermally insulated from and encased in an Inconel vacuum casing to which are attached the graphite tiles which form the inner plasma-facing surface), outer TF, and top and bottom outer PF coils 2, 3, 4, & 5 as shown in the device cross section in Fig. 2. The magnets are powered by phase-controlled rectifier supplies; a motor generator provides the peak feed power (27 kA, 6 kV) needed for operation. The PF 1A and PF 3 coils have bi-polar power supplies and other PF coils are powered by uni-polar supplies. The entire center-stack assembly is fully demountable by removing the TF, OH, and PF 1A connections. The inner TF bundle can be also removed and reinstalled independently from the OH and upper PF 1A assembly. The demountable design therefore provides maintenance, repair, and upgrade opportunities. The TF magnet is designed for and has operated up to 0.6 T at the nominal vessel center $R = 0.86$ m. In 2003, one of the TF coil inner joints failed, which revealed deficiencies of the original design. The failed TF inner conductor bundle was replaced with an improved design in time for the 2004 run.⁽⁹⁾ If a longer pulse or higher field TF magnet is desired in the future, it would be

possible to build an appropriate center-stack and swap the center-stack relatively rapidly (~ 2 months), well within a regular annual outage period.

Vacuum Systems – The NSTX vacuum vessel is roughly a spherical shape, 3 m tall and 3.5 m in diameter, with volume of about 30 m^3 . The plasma volume is $\leq 15 \text{ m}^3$. The vacuum chamber is designed to provide very good plasma access with 12 major ports at the mid-plane between 12 outer TF coil sets. There are two NBI compatible 0.84 m (height) \times 0.74 m (width) rectangular ports; one is currently used for NBI and the other for diagnostics. Three port sections are occupied by the 12 element HHFW antenna systems and one port is dedicated for the vacuum pump duct which presently has two 1600 l/sec turbo-molecular pumps and assorted diagnostics. The remaining six sections each with a 60 cm diameter circular port are mainly utilized for diagnostics. In addition, there are eleven medium size vertical-viewing ports and six smaller ports (horizontal-viewing toward the divertor regions) located on each of the upper and lower dome sections. There are gas feeds installed at three outboard mid-plane locations, one in-board at the mid-plane, one in-board at the “shoulder” near the tip of PF 1A coil, and one in the CHI injector chamber.

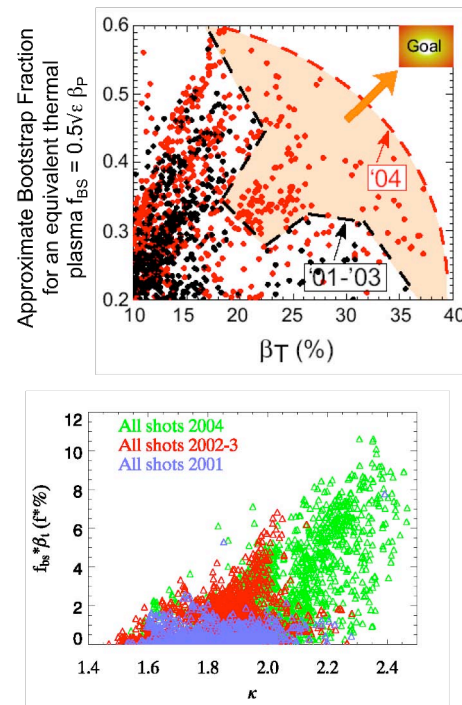


Fig. 3. (a) Achieved parameters in β_T and approximate bootstrap current fraction for an equivalent thermal plasma. (b) Dependence of the product of estimated bootstrap current fraction and toroidal beta β_T on the elongation κ . On both axes of this panel, quantities are averaged over the flattop of the pulse.

Plasma Control System – The real time plasma control system (PCS) on NSTX utilizes a high-speed multi-computer system (SkyBolt II) which processes data from sensors and diagnostic systems in real time to generate commands to the actuators including power supplies and the gas injection system. In 2004,

the PCS response time (or the control latency) was shortened significantly by a factor of 4. This improvement has enabled PCS to control higher elongation plasmas, greatly expanding the operational space as shown in Fig. 3(a). As can be seen from the figure, the higher elongation achieved in 2004 nearly doubled the reactor attractiveness figure of merit given by the product of toroidal beta $\beta_T = 2 \mu_0 \langle p \rangle / B_{T0}^2$ and the nominal bootstrap current fraction, $0.5 \sqrt{\epsilon} \beta_p$ where β_p is the poloidal beta.⁽¹⁰⁾ In Fig. 3(b), the achieved parameters are plotted in β_T and nominal bootstrap current fraction space. As can be seen in the figure, 2004 operation made significant progress toward the eventual goal of reaching the upper right hand corner with simultaneously high $\beta_T \sim 40\%$, and high bootstrap current fraction $\sim 60\%$.⁽¹¹⁾ As the number of actuators for PCS grows, the reliance on the PCS system increases accordingly. In 2004, the rEFIT (a real time plasma equilibrium reconstruction code)⁽¹²⁾ was incorporated into PCS and successfully used in experiments requiring a finer level of plasma shape control and reproducibility. The 2005 PCS development is focusing on optimizing plasma shape with the newly installed new PF 1A coils and controlling the SPA (switching power amplifier) source for the error field and resistive wall mode (EF/RWM) coils (See Sec. 5 for more detail.) The PCS system will continue to evolve with advances in microprocessor technology and also with the availability of new actuators and diagnostic systems.

3. DIAGNOSTIC STATUS AND PLANS

To achieve desired high performance plasmas, it is also crucial to have appropriate plasma diagnostics. Understanding of the physical processes governing the plasma requires detailed information from diagnostics together with the corresponding theory and modeling. For this reason, NSTX has been continuously implementing modern plasma diagnostic systems in key research areas. In this section, we will describe briefly some of the recent diagnostic additions and planned upgrades. A complete list of major diagnostics currently installed and operating on NSTX is shown in Table 1 at the end of this paper. The implementation of diagnostics on NSTX has benefited greatly from collaborations with many national and international institutions.

MPTS, Toroidal CHERS, and other profile diagnostics -In the confinement area, the main effort has been on plasma profile diagnostics. The multi-pulse Thomson scattering (MPTS) system⁽¹³⁾ has 20 spatial channels and two lasers for 60 Hz operation. An upgrade to 30 spatial channels is being implemented in 2005 to give more detailed density and electron temperature spatial information on the H-mode pedestal and internal transport barrier regions. The MPTS system will eventually be upgraded to 45 spatial channels and 3 lasers for 90 Hz operation. The NSTX density profiles are also measured by the microwave reflectometer⁽¹⁴⁾ and the far-infrared laser interferometer and polarimeter⁽¹⁵⁾ (FIRETIP) systems. The toroidal Charge Exchange Recombination Spectroscopy (CHERS) system⁽¹⁶⁾ has been upgraded recently to 51 spatial channels to give detailed ion temperature and plasma toroidal rotation information. With the tangential NBI injection, the NSTX

plasmas can spin toroidally up to ~ 300 km/sec and the Alfvén Mach number ($V_{\text{toroidal}}/V_{\text{Alfvén}}$) can reach as high as 0.5. Typical kinetic profiles for a high- β discharge are shown in Fig. 4. Due to the rapid toroidal rotation, the plasma density tends to peak at further out than the magnetic axis which typically coincides with the peak of the electron temperature. To complement the toroidal CHERS system, an Edge Rotation Diagnostic (ERD) was implemented on NSTX⁽¹⁷⁾ to measure the intrinsic impurity lines from the plasma edge region where the intrinsic line emission is sufficiently strong. ERD can measure both poloidal and toroidal rotation velocities and temperatures. Using ERD, a strong wave-particle interaction was observed which produces significant (~ 400 eV) edge perpendicular ion heating and edge rotation during application of high harmonic fast wave (HHFW) power.⁽¹⁸⁾ The ERD was also used to measure the highly important plasma spin up behavior in the H-mode pedestal region prior to the L-H transition.

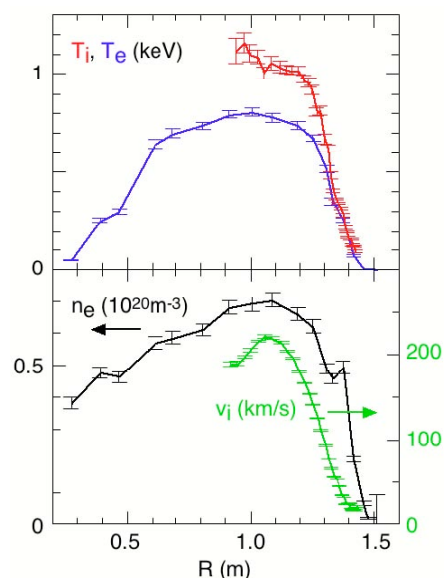


Fig. 4. Measured kinetic profiles of a high beta discharge (shot 112600, 0.55s). (a) T_i profile by 51 spatial channel charge-exchange spectroscopy (CHERS) and T_e profile by 20 channel Thomson scattering (MPTS). (b) Toroidal rotation velocity v_t profile by CHERS and n_e profile by MPTS.

Magnetics and Between-shots EFIT reconstruction - In order to accurately measure the plasma properties at high- β , the NSTX team has implemented a large array of magnetic sensors (poloidal flux loops and pickup coils). Utilizing the magnetic information together with the plasma kinetic profile information (using MPTS and CHERS for the thermal profiles and the energetic population estimated from TRANSP code), a sophisticated plasma reconstruction code “EFIT” has been implemented on NSTX which provides detailed information on the basic plasma properties with time resolution of up to 1 ms.⁽¹⁹⁾ Also a novel plasma diamagnetic measurement has been successfully implemented using the NSTX toroidal field coils which provided valuable inputs into the EFIT reconstruction.⁽²⁰⁾ The EFIT analysis is usually completed in a few minutes after the plasma shot and available before the next plasma shot. In Fig. 5, the EFIT reconstruction incorporating the plasma rotation information for the first time is shown.⁽²¹⁾ Due to the rapid plasma rotation,

the plasma pressure profile is shifted outward from the magnetic axis. The EFIT code has also been linked to the plasma MHD stability analysis code DCON⁽²²⁾ for rapid evaluation of plasma stability.

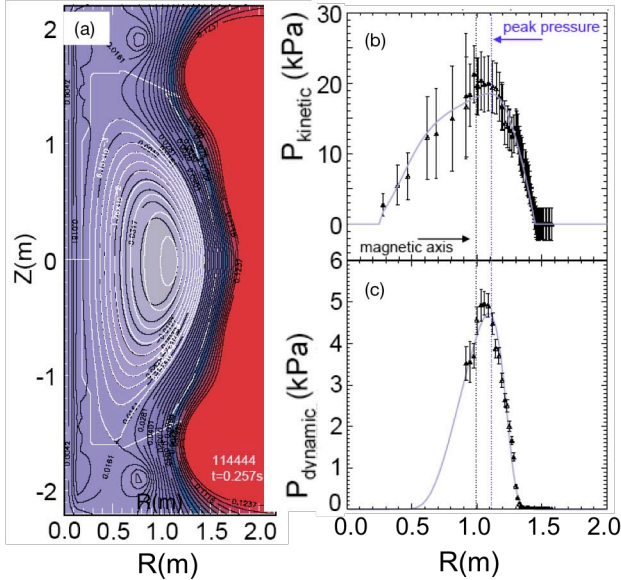


Fig. 5. EFIT plasma equilibrium reconstruction. (a) Plasma pressure (white) and poloidal flux (black) contours. (b) Reconstructed plasma pressure radial profile. (c) Reconstructed dynamic pressure or toroidal rotational kinetic energy density profile.

MSE-CIF System – The MSF-CIF (Motional Stark Effect using Collisionally-Induced Florescence) system⁽²³⁾ was successfully introduced in 2004 to measure the plasma current profile which is crucial for advanced ST operation. The initial four channel data from MSE, which measured the field line pitch in the plasma core, are shown in Fig. 6(a).⁽²⁴⁾ The sensitivity of the pitch angle is excellent even in the relatively low field NSTX plasmas. Indeed, the NSTX MSE-CIF system has achieved a factor of 12 improvement in optical throughput with development of an innovative spectroscopic filter and geometric optimization over earlier high field systems. In addition, higher quantum efficiency detectors provide a further factor of 3.3 improvement in sensitivity. The MSE data has been incorporated into the EFIT analysis and the resulting q profile, shown in Fig 6(b) with 4 channels, has confirmed the existence of a reversed-shear profile in agreement with the earlier inference based on the ultra-soft x-ray data. The MSE also observed periodic variations of the central q and the magnetic axis due to sawtoothing. The MSE system will begin the 2005 run with 8 spatial channels (additional 4 channels) and upgraded toward the full 19 channel system in the near future.

P-CHERS and diagnostics under development - The next step for the plasma profile diagnostic upgrade is the P-CHERS (poloidal-charge-exchange-recombination-spectroscopy) system, which will measure the poloidal rotation information. Together with the toroidal CHERS, a full picture of the plasma flow will then be available. The full plasma flow information combined with other kinetic data will give the radial electric field which will

eliminate the ambiguity in the MSE-CIF measurement associated with the radial electric field. Eventually, a direct measurement of the radial electric field would be highly desirable and to accomplish this an MSE system based on a laser-induced-fluorescence is under development.⁽²⁵⁾ A technique utilizing hypervelocity dust injection (HDI) to measure internal magnetic field vectors at multiple locations simultaneously and to map 2-D and 3-D internal field configurations of NSTX plasmas is also being developed.⁽²⁶⁾ Hypervelocity dust of at least a few micron in radius and a few km/s velocity can reach high temperature regions of the NSTX plasmas according to modeling.

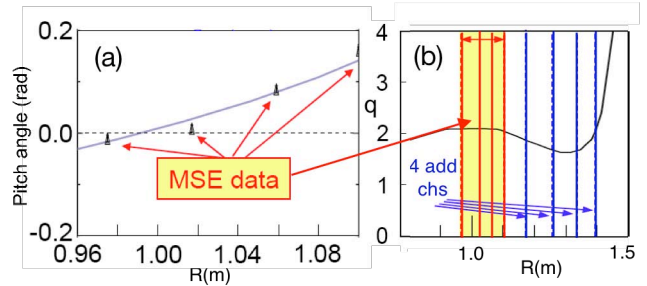


Fig. 6. Initial MSE measurements and EFIT analysis. (a) Measured pitch angle of the local magnetic field vs radius; (b) EFIT reconstruction of the q -profile using the MSE data showing a reversed shear configuration.

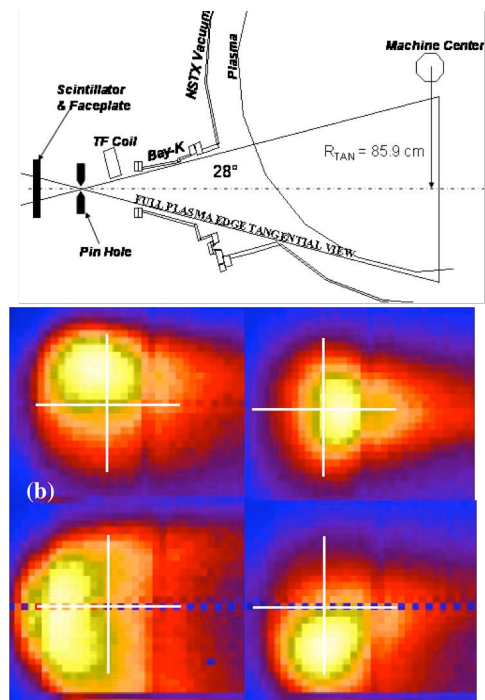


Fig. 7. Fast Tangential Soft X-ray Camera with 64 x 64 pixel image with up 500 kHz, 300 frames based on Princeton Scientific Instruments PSI-5 camera. (a) Schematic view of the fast tangential soft x-ray camera. (b) Initial tangential 2-D images of the $n=1$ tearing mode rotating poloidally around the magnetic axis.

Soft X-Ray Diagnostics - In addition to the high frequency magnetic sensors, ultra-soft x-ray arrays provide information on the MHD activity in the plasma.⁽²⁷⁾ The double-tearing MHD modes observed by the ultra-soft x-ray array suggested the

possibility of the electron transport barriers in the reversed shear plasmas in NSTX. In 2004, a fast tangential soft x-ray camera for 2-D view of core MHD activity with a time resolution down to $2 \mu\text{s}$ was installed (Fig. 7.)⁽²⁸⁾ In Fig. 7(a), a schematic of the camera is shown. The core soft-x-ray (1–5 keV) signal is converted into visible light by a fast phosphor deposited on fiber-optic faceplate. The resulting image is captured by a CCD camera with 64×64 pixels with frame rates up to 500 kHz for 300 frames. Such a camera is a powerful tool to investigate the 2-D MHD mode dynamics including the sawtooth crash. An example of an $n=1$ tearing mode rotating poloidally around the magnetic axis (indicated by the white crosses) is shown in Fig. 7(b).

Fluctuation Diagnostics - To investigate the sources of anomalous transport, a set of core fluctuation diagnostics is being developed. The first element is a microwave reflectometer which can measure longer wavelength fluctuations in the plasma core. Preliminary data have been taken in 2004.⁽²⁹⁾ Far-infrared interferometry is also being used to measure the edge density fluctuations in NSTX.⁽³⁰⁾ A major diagnostic being installed for 2005 is a tangential microwave high- k scattering system to measure the electron-transport-relevant short-wavelength modes including, possibly, Electron-Temperature-Gradient Modes ETGs (Fig. 8).⁽³¹⁾ A schematic drawing of the high- k system is shown in Fig. 8(a). It is designed to measure with a good spatial resolution the spectrum

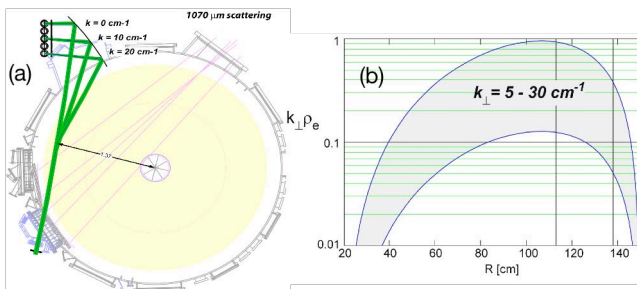


Fig. 8. Microwave tangential high- k scattering system. (a) A schematic view of the high- k scattering system. (b) The normalized accessible wave number range as a function of major radius.

of fluctuations with radial wave number $5 - 30 \text{ cm}^{-1}$ corresponding to modes with $k_{\perp} \rho_e \leq 1$. The accessible normalized wave number range as a function of the major radius is shown in Fig 8(b). This high- k system could be upgraded to gain information on the poloidal component of the wavenumber spectrum. Another system being considered for implementation in the future is a low- k microwave imaging system to reconstruct 2D images of the low- k fluctuations, which may be responsible for the ion energy transport.⁽³²⁻³³⁾

Energetic Ion Loss Detectors - Fast-ion confinement in STs is an important issue, due to the large ratio of their gyro-radius to plasma minor radius. Fast-ion diagnostics on NSTX include a set of neutron detectors, an energetic neutral-particle analyzer (NPA)⁽³⁴⁾, a multi-sightline solid state detector NPA (SSNPA), and a scintillator-based fast lost-ion probe (sFLIP).⁽³⁵⁾ Since the DD fusion neutron rate in NSTX is dominated by beam-target

reactions, the neutron measurements provide a global measure of beam ion confinement. The detectors include two absolutely-calibrated fission chambers and four scintillator detectors capable of resolving fluctuations in the neutron rate up to 100 kHz. The neutron response produced by short neutral beam pulses has shown classically-expected beam ion confinement in quiescent plasmas.⁽³⁶⁾ The NPA can measure fast neutrals with energies up to 120 keV with an energy resolution of $\sim 1 \text{ keV}$, and can be scanned horizontally and vertically on a shot-to-shot basis. The NPA measures the fast ion population at the point of charge exchange. The ability to look at the fast ion population in the core of the plasma is greatly enhanced by the NBI providing the source of neutrals. The SSNPA has four fixed sightlines in the mid-plane with $\sim 10 \text{ keV}$ energy resolution and is designed to measure radial redistribution of neutral beam ions arising from MHD activity. The sFLIP measures the energy and pitch angle of the escaping fast ions entering the detector, allowing determination of the orbits that are lost. Initial sFLIP measurements also appear consistent with classically-expected confinement in quiescent plasmas. However, MHD activity has been seen by the NPA to deplete the confined beam ion population and result in loss to the vessel wall of orbits with high pitch angle.⁽³⁷⁾ A neutron collimator system is being designed to quantify the fast ion population in the plasma core region.

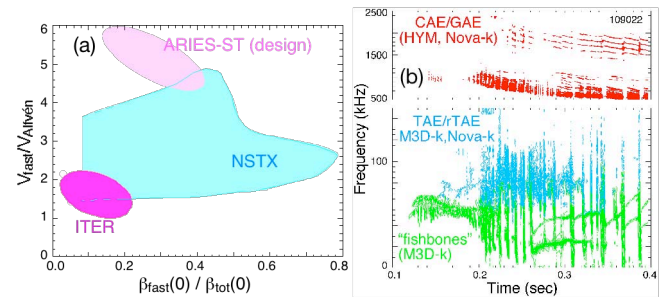


Fig. 9. Energetic-ion-induced instabilities. (a) Normalized energetic ion velocity and beta parameter space for NSTX and projected ITER and ARIES-ST regimes. (b) Energetic-ion-induced MHD instabilities observed in NSTX.

Energetic-Particle-Driven Instabilities - Because of the high β of NSTX plasmas, the Alfvén wave velocity approaches the bulk ion velocity. With energetic NBI heating, it is possible to access the plasma regimes where the fast ion velocity exceeds the local Alfvén velocity. This condition is expected in burning plasmas due to the presence of 3.5 MeV fusion alpha (helium) particles. The alpha driven high frequency MHD instabilities could cause anomalous alpha particle diffusion and loss from the burning plasmas. In Fig. 9(a), the NSTX experimental regimes as well as the expected operating regimes of ITER and an ST-reactor are indicated in the Alfvén Mach-number and the normalized fast-ion pressure parameter space. As can be seen in Fig. 9(a), with the high Mach number of the high power NBI beam ions, NSTX can explore a wide range of Alfvén Mach number and the beam ion pressure fraction. For the high frequency MHD studies, the high frequency magnetic sensors with up to 2 MHz response are operational on NSTX. Typically observed high frequency MHD instabilities including TAEs (Toroidal Alfvén Eigenmodes) and CAEs (Compressional Alfvén Eigenmodes) are shown in Fig.

9(b).⁽³⁸⁻³⁹⁾ These observed modes were reproduced by the kinetic high frequency MHD codes HYM, Nova-K and M3D-k. The microwave reflectometer and FIRETIP are also used to detect the high frequency MHD modes in the core.

Boundary Physics Diagnostics - For edge/divertor research, a fast reciprocating Langmuir probe is operational which can measure a variety of plasma parameters including density, temperature, fluctuations, and flow information at the mid-plane through the scrape-off layer and to about 5 cm inside the last closed flux surface.⁽⁴⁰⁾ A powerful tool for the edge fluctuations is the gas-puff imaging (GPI) system, shown in Fig. 10(a) which can capture images of edge fluctuations with time resolution down

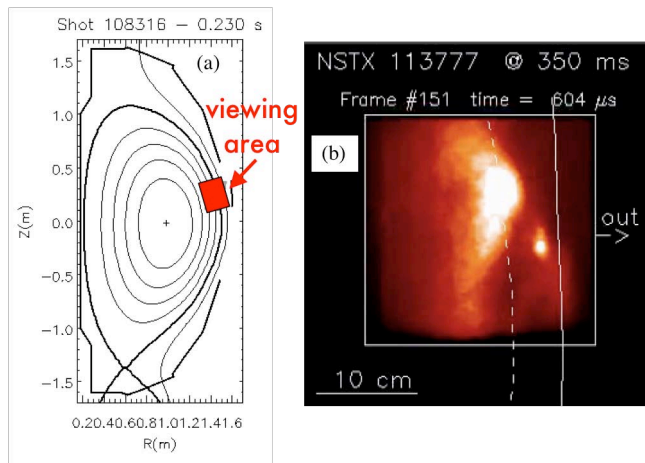


Fig. 10. Gas Puff Imaging Diagnostic. (a) Viewing area of ~ 25 cm x 25 cm with spatial resolution of ~ 1 - 2 cm. The camera is Princeton Scientific Instruments PSI-5 camera with 250,000frames .sec with 64 x 64 pixels/frame. (b) A captured image of a “blob” moving radially out across the plasma edge region.

to 2 μ s.⁽⁴¹⁾ The GPI system has revealed images of “blobs” coming out of the plasma. These represent a highly non-linear but apparently ubiquitous form of the edge fluctuations and energy transport [Fig. 10(b)]. Another fast visible camera viewing tangentially in the divertor region⁽⁴²⁾ has revealed a variety of interesting ELM behavior including new Type-V ELMs, which cause minimal plasma energy losses.⁽⁴³⁾ In the area of the edge power flow to plasma facing components (PFCs), three infrared (IR) cameras are monitoring the power flow to the divertor and wall surfaces. A faster IR camera will be installed to capture the transient energy flow during fast MHD events such as ELMs. Surface monitoring tools such as wall coupons have been employed on NSTX since the start of the operation. Recently in-situ wall condition measuring diagnostics have been introduced including surface deposition monitors and a novel dust detector with a sensitivity better than 1 μ g/cm².⁽⁴⁴⁾ The surface deposition of dust and other material is of particular interest to future long pulse devices such as ITER and CTF.

4. NSTX FACILITY TOOLS AND UPGRADE PLAN

In order to improve the quality of the plasma toward what is needed for our long range research goals, NSTX has been implementing and improving a number of research tools as the areas of fueling, wall conditioning, power and particle handling, heating and current drive, and solenoid-free start-up.

Advanced Fueling Tools - The gas injection at the outboard side of the spherical torus tends to have rather poor fueling efficiency of $\leq 10\%$ in diverted discharges due to the very short connection length from the mid-plane to the divertor region. This inefficiency necessitates strong gas injection which increases the gas loading of the walls as the NSTX graphite PFCs absorb the deuterium working gas. As the plasma transitions into an H-mode, a rapid density build up takes place in the particle transport barrier region resulting in a hollow density profile. Following the rapid build up of the edge density, there is a gradual density build up in the core and the average density often approaches the Greenwald density limit during a long-pulse high performance discharge. For advanced long-pulse non-inductively sustained plasmas, which need efficient non-inductive current drive, it is desirable to keep the plasma density lower since the non-inductive current drive efficiency goes up with increased electron temperature and reduced plasma density. In tokamak experiments, reduced particle recycling has also led to improved confinement and plasma performance in some cases. So, as the NSTX research is focusing toward the long-pulse non-inductive regime, improving the fueling efficiency is of strong interest. Gas injection at the inboard side of the plasma has been tested,⁽⁴⁵⁾ and while no significant fueling efficiency improvement was observed, the inboard gas injection appears to improve access to the H-mode.⁽⁴⁶⁾ Recently, a supersonic gas injector with up to Mach 7 capability has been developed and tested on NSTX.⁽⁴⁷⁾ This injector is located at the outer mid-plane, as shown in Fig. 11(a). A fast visible camera picture during the injection, Fig. 11(b), shows a relatively narrow gas plume, consistent with a simulation. The initial test indicated significantly higher fueling efficiency. The supersonic gas injector will be further tested in 2005. An injector for solid deuterium pellets is being considered for core fueling in the future. A Compact Torus (CT) injector is also viewed as a promising fueling method with application to a future reactor, particularly for STs since the strong toroidal field gradient will produce a radially localized deposition of particles from the injected CTs.⁽⁴⁸⁾

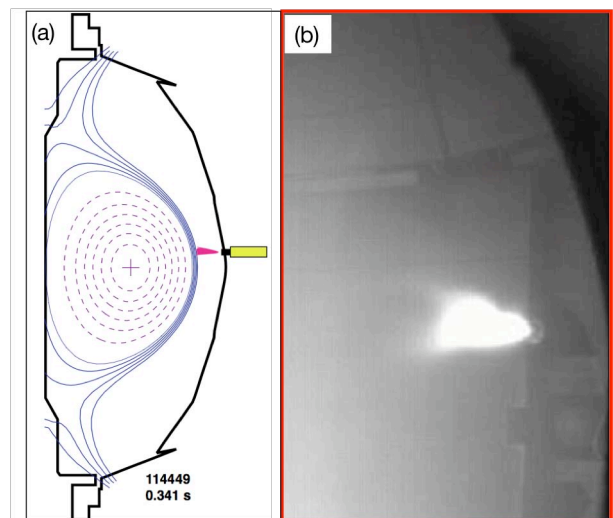


Fig. 11. Supersonic Gas Injector. (a) A schematic of the supersonic gas injector placed in the outer mid-plane. (b) A fast camera image of the supersonic gas injector showing **Impurity Control and Wall Conditioning Tools** – The plasma

contacting wall surfaces in the NSTX vacuum chamber are lined with graphite tiles to eliminate metallic impurities. To minimize the water trapped in them after a vacuum opening, the carbon tiles are baked up to 350°C for a period of several days. The elimination of absorbed water is very important to reduce both the oxygen and hydrogen levels. To reduce these oxygen levels further, wall boronization is performed using deuterated trimethylboron (TMB) gas mixed into helium glow discharges.⁽⁴⁹⁾ The boronization also reduces the hydrogen level which is desirable to reduce the hydrogen minority absorption during HHFW heating. With boronizations, the hydrogen to deuterium ratio during a plasma discharge can be reduced to a few % level and often even below 1% as shown in Fig. 12. The boronization on NSTX can be performed during the high temperature bake after a vacuum opening and during plasma operation, weekly, daily or even between plasma shots, if desired. To minimize the deuterium inventory in the carbon tiles, a helium glow discharge is created by applying a bias voltage between a glow probe and the vacuum vessel for 10 – 15 minutes between plasma shots. Such a glow removes the hydrogenic gases trapped in the graphite surfaces, reducing the uncontrolled density rise and making more reproducible discharges. The glow discharge system is now being upgraded to make the glow probe which was fixed in the shadow of the limiter to a movable one so that the glow can fill the entire vessel to improve the wall coverage for 2005.

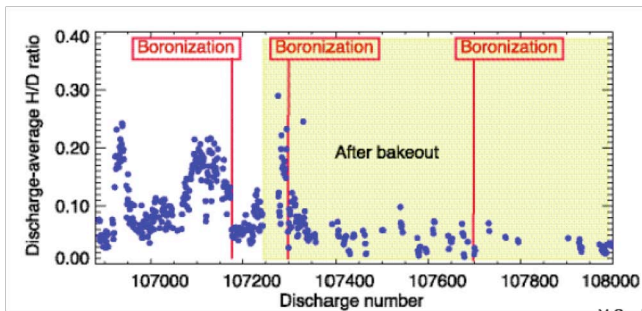


Fig. 12. Evolution of H/D ratio as a function of the plasma discharges showing a general reduction after bakeout and boronization.

Tools for Power and Particle Control – In addition to developing efficient particle fueling, developing an efficient particle pumping (removal) tool is an important research topic for reaching long-pulse, non-inductively sustained, high- β plasmas. The helium glow is effective in removing the hydrogen particles from the surface of the graphite wall which provides a limited pumping capacity. However, we will eventually need a larger capacity pumping system for longer pulse discharges. A cryo-pump placed in the closed divertor region is being considered for NSTX. This approach is already pursued on many tokamak devices and can be applied to NSTX in a relatively straightforward manner. Presently, the NSTX team is also testing particle control based on lithium which is unique to NSTX among the presently operating large facilities. The lithium approach has been successfully used on TFTR and is also being tested on smaller facilities, such as CDX-U.⁽⁵⁰⁾ Lithium coatings have been used previously for wall-limited (Supershots) plasmas in TFTR to improve the plasma performance. An important question being pursued on NSTX is whether the lithium approach would be

equally effective in diverted H-mode discharges. The first approach being introduced on NSTX is a lithium pellet injector which is designed to inject up to eight 1 – 5 mg solid lithium pellets into a given discharge with speed of up to 200 m/s. In the 2004 run, a preliminary test was performed with total of 17 pellets of about 2 mg each injected into sixteen plasma discharges.⁽⁵¹⁾ During a double-null divertor NBI heated discharge, the injected lithium was transported relatively uniformly to both top and bottom divertor regions as indicated by the picture taken in neutral lithium light shown in Fig. 13(a). In Fig 13(b) the oxygen level (monitored in the early phase of OH discharge when the discharge conditions are similar) is plotted against the integrated amount of injected lithium and shows a monotonic decrease. The lithium

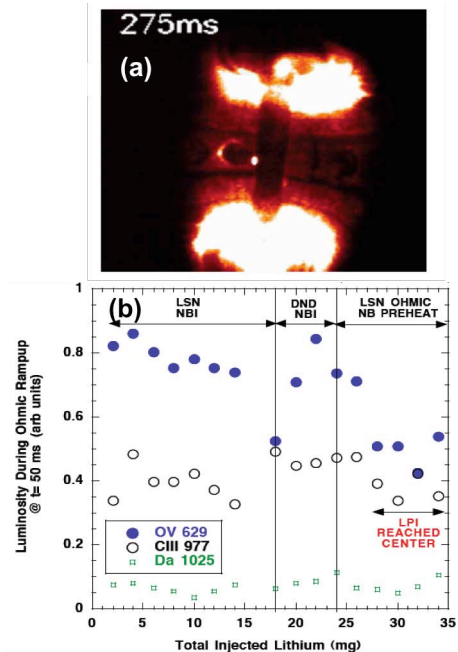


Fig. 13. (a) A fast camera image in neutral lithium emission following injection of a lithium pellet into a double null divertor discharge. (b) Impurity emission measured during the discharge startup as a function of the cumulative lithium injection showing downward trend for the oxygen impurity.

The different plasma conditions are indicated as follows - LSN:

lower single null divertor, DND:double null divertor.

pellet injection experiments will continue in 2005. As a next step, a lithium evaporator is planned in 2006 in collaboration with CDX-U. The evaporator is designed to coat the existing divertor graphite tile surfaces. The material of the coated surface may be changed to improve the lithium pumping efficiency. For a longer term development, a liquid metal module which will be placed at the bottom of the vessel in the outer divertor strike point region is being considered in collaboration with VLT (the Virtual Laboratory of Technology). The initial liquid lithium experiment on CDX-U has been quite encouraging in terms of drastically reducing the oxygen level and the particle recycling. Such a liquid metal module has the potential of being able to manage the intense heat flux as well as controlling particle recycling in the steady-state condition expected in future high-heat-flux fusion devices such as CTF and Demo.

Heating and Current Drive Systems – The two main heating and current drive systems on NSTX are Neutral Beam Injection (NBI) and High Harmonic Fast Wave (HHFW) RF power. The NSTX NBI system utilizes the well developed TFTR NBI system.⁽⁵²⁾ The NSTX NBI system has delivered up to 7 MW at an acceleration voltage up to 100 kV and it is the workhorse of the NSTX high- β high-performance plasma research. There are three ion sources with tangency radii 70 cm, 60 cm, and 50 cm. The beam system is a reliable means of plasma heating but it also serves other important functions: to impart toroidal momentum to induce strong toroidal plasma rotation of up to ~ 300 km/s; to drive plasma current (in addition to the bootstrap current) of up to ~ 200 kA; to provide an energetic ion population for simulating alpha-particles (Sec. 3); and to support plasma profile diagnostics such as CHERS and MSE (Sec. 3.)

The HHFW system utilizes 6 high-power transmitters connected to a twelve-element antenna system for a total delivered power of 6 MW at 30 MHz. The NSTX HHFW system was originally used for the ICRF experiments on TFTR. The main purpose of the HHFW system is to heat electrons and drive plasma currents for non-inductive current sustainment.⁽⁵³⁾ The HHFW system is also planned to be used to start-up and ramp-up the plasma current. It has also been used for pre-ionization during the PF-only start-up experiments. The system is designed to be able to vary the relative phases of the six transmitters in real time, to change the phase velocity or, equivalently, the toroidal wavenumber k of the launcher wave. This capability is required to track the plasma evolution from a few 100eV in OH plasmas at the start-up to a few keV in the heated phase. When the antenna elements are phased to launch a traveling wave, they are capable of driving plasma current of a few hundred kA. The HHFW has heated the core electrons from the few hundred eV typical in the ohmic phase to typically ~ 2 keV (up to 3.8 keV achieved.) and initial

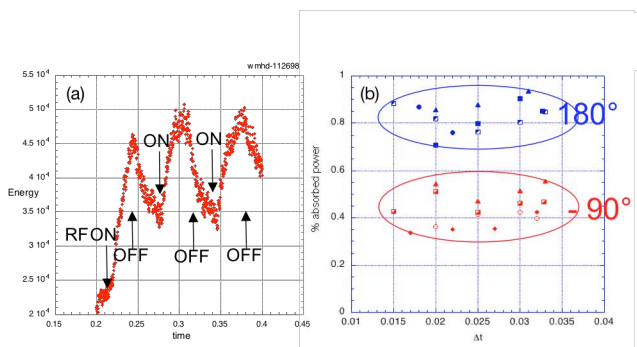


Fig. 14. HHFW modulation experiments for heating efficiency.

(a) Temporal evolution of measured plasma stored energy (EFIT). The square wave HHFW power on-off times are indicated. (b) Measured heating efficiency for slow heating phasing (inter-strap phase difference 180° , $k \approx 14\text{m}^{-1}$), and the faster current drive phasing (phase difference 90° , $k \approx 7\text{m}^{-1}$).

experiments on current drive have been performed.⁽⁵⁴⁾ However, the efficiency of HHFW heating appears to be rather variable. Modulation experiments [Fig. 14(a)] show a relatively good heating efficiency of $\sim 80\%$ with a slow heating phase of $k \sim 14\text{m}^{-1}$, (180° strap to strap phase difference) but the heating efficiency is significantly reduced to $\sim 40\%$ for $k \sim 7\text{m}^{-1}$ (-90°)

[Fig. 14(b)] and little heating was observed for the fastest phase with $k \sim 2.5\text{m}^{-1}$ (-30°).⁽⁵⁵⁾ Interestingly, relatively higher heating efficiency $\sim 70\%$ was observed for $k \sim 7\text{m}^{-1}$ (90°). At the same time, strong ion heating was observed in the edge which appears to be correlated with a parametric decay of the launched wave into ion Bernstein waves and an ion quasi-mode. Investigation of this and efficiency optimization will be important topics of the near term HHFW research. While the present HHFW antenna system has reached the design value of 6 MW, it has suffered from transient RF breakdown at powers above 4 MW. The observed break down voltage across the insulators in the RF feed-thrus is considerably lower in NSTX than TFTR, probably caused by increased cross-field particle diffusion into the feed-thru region as a result of the lower toroidal field of NSTX. A possible solution is to upgrade the antenna to a symmetric-feed configuration which will increase the coupled power level by a factor of two for a given feed-thru voltage. The symmetric antenna also moves the current maximum point, which corresponds to the point of maximum radiation, to the mid-plane from the end of the antenna; this would be beneficial from the wave physics and operational points of view.

Solenoid-Free Start-Up Systems – The solenoid-free start-up is an important component of NSTX research since ST reactors such as CTF and ARIES-ST assume no ohmic solenoid. Advanced tokamak reactors such as ARIES-AT are also designed without ohmic solenoid. On NSTX, the Coaxial Helicity Injection (CHI), which was developed on the HIT devices, is being pursued as a means for solenoid-free start-up.⁽⁵⁵⁾ In NSX using a rectifier supply, CHI has generated up to 400 kA of toroidal current and a

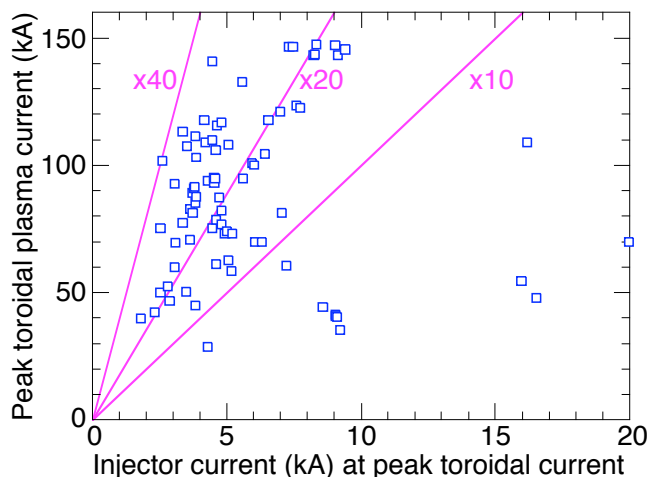


Fig. 15. Toroidal plasma current vs injected current using transient CHI. The lines indicate the current multiplication factors, as labeled.

current multiplication of up to 14 has been obtained. However, it was difficult to assess how much of the toroidal current was actually flowing in the closed flux surfaces. Recently on HIT-II, a new technique called a “transient” CHI was developed which successfully produced high-quality “closed flux” discharges. By utilizing relatively short injection pulses, it was found to be possible to “detach” the plasma current ring from the injector to create flux closure. By initiating the plasma with the transient CHI technique, the performance of the plasma during the

subsequent inductive phase was significantly improved, resulting in volt-second savings and significantly higher plasma current. On NSTX, in 2004, a capacitor bank was commissioned to test this concept. Initial experimental results at 1 kV bias voltage were encouraging, producing about 150 kA with a few kA of injected current, yielding current multiplication factors of as high as 40, as shown in Fig. 15. In preparation for the 2005 run, the transient CHI injector was improved to allow direct gas-feed to allow breakdown with reduced gas input to the main chamber. In addition, the ECH pre-ionization will be introduced directly into the injector to create a “seed” plasma to “bubble-up” into the main chamber, trapping the injector poloidal flux.

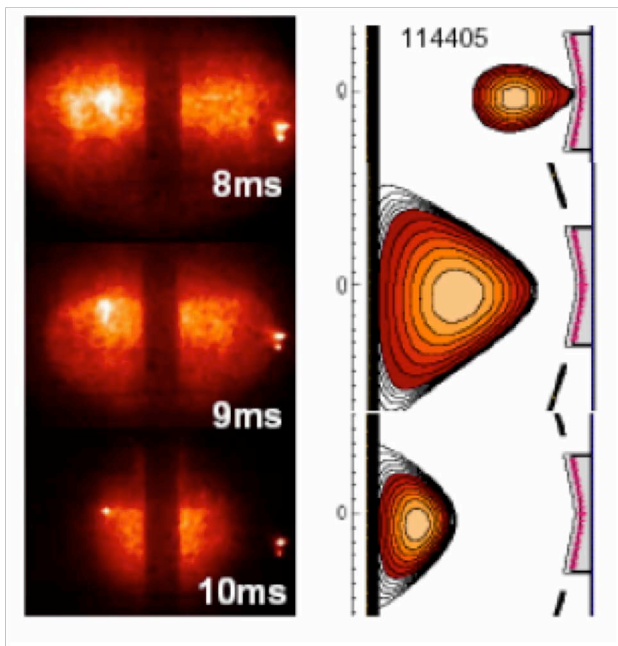


Fig. 16. Outer PF-Only Solenoid-Free Start-up. (a) Fast camera images of the toroidal current ring. (b) Corresponding reconstructed plasma current ring evolution.

In parallel to CHI, the NSTX team is pursuing another solenoid-free approach utilizing the outer PF coils. There are several variations of the outer-PF-only plasma start-up approach. On the JT-60U and TST-2 devices, significant plasma currents of up to 150 kA were generated by the simple vertical field swing in the presence of strong ECH heating.⁽⁵⁷⁾ In addition to the TST-2/JT-60U technique, a merging plasma ring approach developed on TS3/4⁽⁵⁸⁾ has been successfully demonstrated on the MAST device recently.⁽⁵⁹⁾ A poloidal flux / field-null optimized scenario is also being developed for NSST.⁽⁶⁰⁾ On NSTX, the outer-PF-only plasma start-up was tested in 2004 without the strong ECH applied. Using HHFW as a pre-ionization source, a successful start-up was demonstrated producing ~ 20 kA of toroidal current, but only when a very good field-null condition was satisfied. Without ECH, the start-up condition appeared to be rather stringent. The plasma images from the fast visible camera are shown in Fig. 16(a). The pressure profiles measured by MPTS peaked at the locations consistent with the plasma images. A plasma simulation of the corresponding discharge is shown in Fig. 16(b) where pertinent discharge features are reproduced. In order to allow less stringent field null conditions, a high power ECH source would be required as demonstrated in

TST-2 and JT-60U. Other alternatives such as plasma gun and CT injection are being considered to provide a suitable target plasma for the start-up.

5. NEW TOOLS FOR ADVANCED ST OPERATIONS

Because of the favorable MHD stability at low aspect ratio $A=R/a < 2$, the NSTX has already accessed high average toroidal beta of 35-40% and central beta of order unity at high plasma current of ~ 1.3 MA at keV range temperatures. The Troyon normalized beta, $\beta_N = \beta_T a B_T / I_p$, has exceeded $6 \% \cdot \text{m} \cdot \text{T} / \text{MA}$ in the NSTX discharges. This high toroidal beta permits fusion power production at a relative moderate confining toroidal field thereby reducing the power plant cost. The unity beta condition is also relevant for the physics of space plasmas. The high β_N discharges have high bootstrap-current fraction which is desirable for non-inductively sustained reactor operation. However, to be truly reactor relevant, it is necessary to have high- β and high bootstrap current fraction simultaneously as indicated in Fig. 3(b).

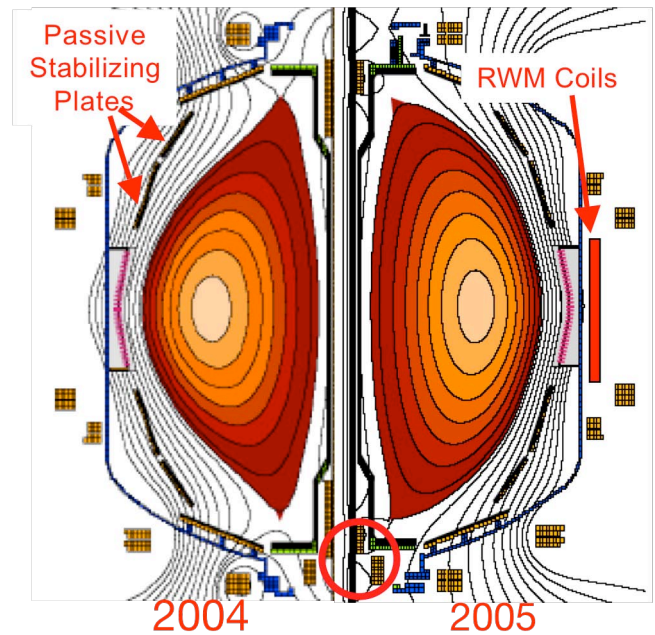


Fig. 17. PF 1A upgrade. The left panel is the old configuration and the right panel is the new configuration ($\kappa = 2.5$, $\delta = 0.8$) implemented in 2005. By shortening the PF 1A coils, it will be possible to provide finer plasma shape control at high elongation and to sustain the higher bootstrap current fraction needed for advanced operation.

Two major new tools are introduced in 2005 for MHD control. The first is a new pair of PF 1A coils to give greater plasma shaping capability to access high- β , high-bootstrap-current regimes. The second is a set of Error Field/Resistive Wall Mode coils powered by Switching Power Supplies (SPA) to enable operation near the ideal MHD stability limits. Another possibility for the future is current profile control provided by Electron Bernstein Wave (EBW) current drive. A finer current profile control is expected to become increasingly critical as the plasma approaches the ideal MHD stability limits. An EBW system is planned as a high priority upgrade for NSTX.

However its implementation is contingent upon the availability of the funding.

New PF 1A Coils - The NSTX experimental results and recent modeling of advanced ST discharge scenarios predict that strong plasma shaping (higher elongation and high triangularity) is important to achieve simultaneous high- β , high-bootstrap-current discharges. The original PF 1A coils were designed for plasma elongations $\kappa \sim 2$. Despite this, these coils have been used successfully to achieve high elongation plasmas as discussed in Sec. 2.2 and shown in the left panel of Fig. 17. However, the solenoid-like PF 1A coils made precise shape control at high elongation difficult. A study showed that shorter PF 1A coils (shown as a circle) can produce high triangularity at high elongation as shown by the right panel in Fig. 17. The new plasma shape also conforms more closely to the passive stabilizer plates which is more favorable for wall stabilization. The resulting plasmas are predicted to have $\beta_T \sim 40\%$, with high bootstrap current fraction of $\sim 60\%$ under optimized pressure profiles. Thus, new PF 1A coils were fabricated and installed on NSTX for the 2005 plasma operations.

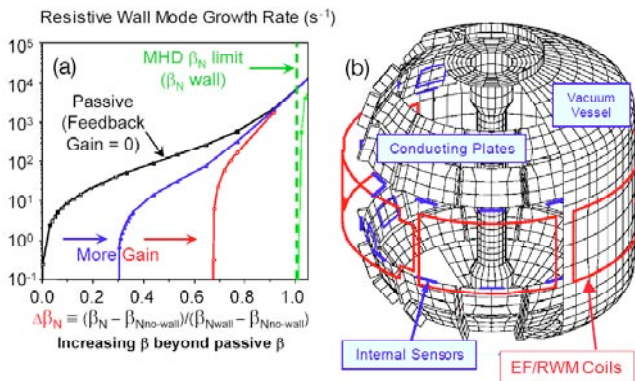


Fig. 18. Error Field / Resistive Wall Mode Control Coils powered by fast Switching Power Amplifiers. (a) The estimated RWM growth rate for various feedback gains enabling the stable operations well above the no-wall beta limit (Gain = 0). (b) A schematic of the RWM coils on NSTX in red. The RWM magnetic sensors embedded in the passive plates are shown in blue.

Error Field/Resistive Wall Mode Coils – As the plasma β increases above the non-wall-stabilized MHD β limit, it is important to have methods to control the MHD mode growth. There are two fundamental approaches being tested on NSTX. Sufficient plasma rotation together with a nearby conducting wall is predicted to stabilize the ideal MHD kink/ballooning mode.⁽⁶¹⁾ However, below a critical rotation frequency, the resistive wall mode (RWM), a kink mode modified by the presence of a conducting wall, can become unstable and grow, leading to rapid rotation damping and beta collapse on the timescale of the decay of wall eddy currents.⁽⁶²⁾ Such unstable modes appear to preferentially grow from perturbations caused by the intrinsic error fields which act as the “seeds”. In 2002, the plasma beta values were improved significantly by reducing the intrinsic error fields by realigning the PF-5 coils.⁽⁶³⁾ With sufficient plasma rotation, the β limit of NSTX plasmas have significantly exceeded

the no-wall limits for many resistive wall times demonstrating the effectiveness of wall stabilization. Further progress is expected by actively canceling the error field growth using externally installed EF/RWM coils as demonstrated on DIII-D.⁽⁶⁴⁾ This approach will be investigated in 2005.

The second approach is a direct feed-back stabilization of the growing RWM using the external coils connected to the SPA supply under the control of the real-time plasma control system. While the wall stabilization with plasma rotation is a simpler approach, this feed-back control method maybe needed if a sufficient plasma rotation for the wall stabilization is not practical in a reactor. The calculated RWM growth rates are plotted in Fig. 18(a) for various gains in a feedback loop showing that stable operation well above the zero gain case (no-wall beta limit) should be achievable. This approach would enable operation near the ideal MHD limit without requiring the plasma rotation, which is more desirable from the reactor point of view. On NSTX, both approaches will be investigated. The error field control is technically easier to implement so it will be tested first. As the feedback control capability is improved through testing, the direct feedback stabilization of RWMs will be attempted.

The NSTX EF/RWM Coil System consists of six “picture frame” coils mounted outside but close to the vacuum vessel near the outboard mid-plane as shown in Fig. 18(b). The coils are configured as three opposing pairs to generate a radial field and each coil pair is powered independently by a fast switching power amplifier (SPA). In order to investigate the behavior of resistive wall modes, a resistive wall-mode sensor system has been implemented which can detect $n = 1, 2, \& 3$ modes with high sensitivity. The RWM coil sensors are embedded in the passive plates and shown in blue in Fig. 18(b).⁽⁶⁵⁾ Two of the coils were installed during the 2004 experimental campaign and powered by a slower rectifier supply to modify the intrinsic error fields. The initial operation of the partial EF/RWM coils showed that the locked-mode density threshold could be reduced significantly by reducing the intrinsic error fields. The RWM physics and the effect of error fields on the plasma toroidal rotation were also investigated. In 2005, the experimental campaign with a full set of EF/RWM coils powered by SPA will begin. With the EF/RWM coil system, NSTX will investigate operation at high β well beyond the “no-wall” MHD β limit and approaching the ideal wall stabilized MHD β limit.

Electron Bernstein Waves for Current-Profile Control – Control of current profile is a crucial capability to optimize the β limit of advanced ST (and tokamak) discharges. Calculations predict that the required current drive location is for $r/a > 0.6$, to achieve rather broad current profiles needed for MHD stability. For NSTX, the advanced scenarios suggest about 100 kA of off-axis current is needed to be driven at $r/a \sim 0.7$.⁽⁶⁶⁾ Because of the large trapped particle fraction in this region, the conventional current drive efficiency is expected to go down rapidly with minor radius. In addition, due to the relatively low magnetic field, the ST plasma core is over-dense (inaccessible) for conventional electron cyclotron current drive (ECCD.) NSTX is therefore examining a new type of current drive using Electron Bernstein Waves (EBW.) The electrostatic EBW has essentially no density limit so it can freely access the high density, high dielectric plasma core of NSTX.⁽⁶⁷⁾ At the electron cyclotron harmonic

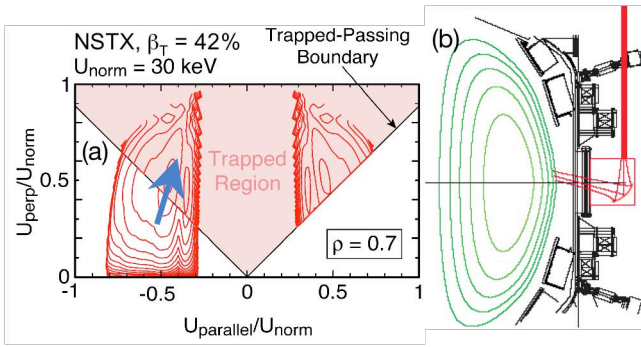


Fig. 19. Current profile control with electron Bernstein waves (EBW). (a) Efficient off-axis current drive using unidirectionally launched EBW to move the passing particles into the trapped region. (b) A schematic of a conceptual EBW launcher on NSTX

resonance, EBW can be absorbed strongly. What makes EBW particularly attractive is the high current drive efficiency predicted at larger values of r/a due to the “Ohkawa” current. Because of strong perpendicular heating, the EBW can accelerate passing electrons into trapped orbits as depicted in Fig. 19(a). By preferentially heating the passing particles moving in one direction into trapped orbits, EBW can effectively remove the plasma current thus it can induce a net current change. The effectiveness of the Ohkawa current tends to increase with larger trapping fraction or larger r/a . It is estimated that in NSTX about 3 MW of EBW power is needed to drive the required 100 kA of off-axis current in the advanced high- β ST regime. NSTX is currently investigating the EBW coupling physics through the EBW emission measurements. A promising EBW scenario is identified at 28 GHz with the O-X-B coupling scenario where the EBW emission measurements suggests an efficient coupling of EBW for this scenario.⁽⁶⁸⁾ O-X-B coupling appears to be more suitable for high power EBW experiments since it is only mildly sensitive to variation in the edge density gradient and the coupling resiliency can be further improved by polarization adjustments. NSTX plans to develop a 1 MW 28 GHz EBW system as at high priority in the near future. Meanwhile, EBW emission measurements are being conducted on NSTX to assess the EBW power coupling efficiency. A schematic of the 1 MW EBW launcher is shown in Fig. 19(b).

6. NEXT-STEP SPHERICAL TORUS

6.1. ST Development Path – An effective and accelerated development of fusion energy using key contributions from the ST is envisioned in Fig. 20.⁽⁴⁾ In the ST development path, considering the limited world-wide availability of tritium in the foreseeable future, an ST-based compact Component Test Facility (CTF) with fusion power level of < 200 MW is envisioned to complement ITER to develop reliable core components for Demo. The ST-based compact CTF, even with a relatively modest fusion power, can provide sufficient neutron flux and fluence to meet the

blanket R&D needs. As illustrated in Fig. 20, the ST development path starts with the on-going $I_p \sim 1$ MA level ST experiments (e.g., NSTX, MAST) to establish the physics principles of the ST concept. The Next-Step ST (NSST) with $I_p = 5-10$ MA is needed to provide the ST physics database at fusion plasma parameters, including physics of alpha-particles at high- β with significant fusion gain of $Q \geq 2$. Early in its operation, NSST will develop physics basis needed to design and construct a compact CTF device without an ohmic solenoid. This includes a demonstration of multi-MA solenoid-free start-up and non-inductive sustainment. Once the CTF physics feasibility demonstration is achieved on NSST, the CTF engineering design and construction can proceed at a separate nuclear site. The

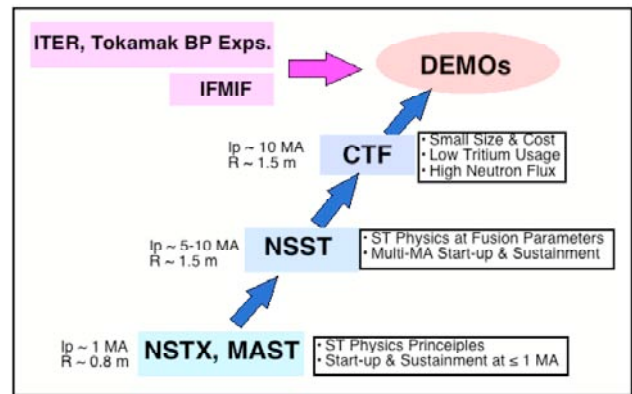


Fig. 20. ST contribution to the fusion energy development path complementing ITER-BP/IFMIF. The present experimental devices including NSTX/MAST provide physics data base for the design of NSST. The NSST operating at 5 – 10 MA at fusion parameters provides necessary physics basis for CTF and high beta physics data for Demo. The CTF facility is dedicated to develop high performance reliable core components for Demo.

NSST facility can then continue to explore more advanced ST regimes to optimize the plasma performance for CTF and help design an attractive Demo. The ST development path via CTF would therefore complements the tokamak burning plasma experiments such as ITER.

6.2. NSST Mission –NSST is envisioned ST with $I_p \times A \approx 8 - 16$ MA, which is similar in performance as to tokamaks such as JET, JT-60, and TFTR.⁽⁴⁾ The primary mission elements of NSST are to conduct spherical torus research at fusion plasma parameters to

- Explore advanced physics and operating scenarios with high bootstrap current fraction / high performance sustained advanced ST regimes, which can be utilized on CTF and DEMO,
- Provide sufficient physics basis for the design of a compact CTF, and
- Contribute to the general plasma / fusion science of high β toroidal plasmas including astrophysics.

The NSST is envisioned to complement ITER as it will provide a database on important issues for burning plasmas such as alpha physics in higher beta regimes not covered by ITER to design an attractive DEMO.

6.3 Base Physics Design Parameters of NSST - To guide in the selection of a design point, which can meet the requirements of the NSST mission, a systems code was developed and a parametric study has been performed. Many promising design points have emerged. The Tokamak Simulation (TSC) Code was also used to validate the systems-code findings. The current sustainment regime at $B_T = 1.7$ T (τ -pulse = 20 sec $\sim 3 \tau$ -skin) is ideal for investigating the CTF-like regimes at moderate Q . Here, a half-swing of the ohmic heating (OH) coil (from initial pre-charge current ramped down to zero) can start up the plasma. Another important research aim of NSST is to demonstrate multi-MA non-inductive start-up which is essential to establish a design base for a toroidal CTF without an ohmic heating solenoid. To allow sufficient pulse time to investigate such non-inductive scenarios, NSST can operate for 50 s at 6 MA with $B_T = 1.1$ T. Finally, to explore a wider ST plasma-parameter space, the NSST device can operate in a purely inductive mode up to 10 MA with $B_T = 2.7$ T with a 5 s flat-top using the full OH swing, where $Q = 2$ performance can be expected with an enhancement of confinement over the ITER H-mode confinement scaling [ref.], $H_{H97} = 1.4$. This operating mode will enable an exploration of α -particle related physics in high β plasmas for τ -pulse $\sim 5 \tau_E$. A TSC simulation for the 10 MA inductive case has yielded $Q \sim 2$ with somewhat relaxed $H_H = 1.3$. The plasma energy confinement is being investigated on NSTX.⁽¹¹⁾ The confinement behavior in NSTX appears to be more strongly dependent on the toroidal magnetic field than the conventional scaling where higher confinement enhancement factor of up to ~ 1.3 have been seen at $B_T = 4.5$ kG while the confinement enhancement is significantly

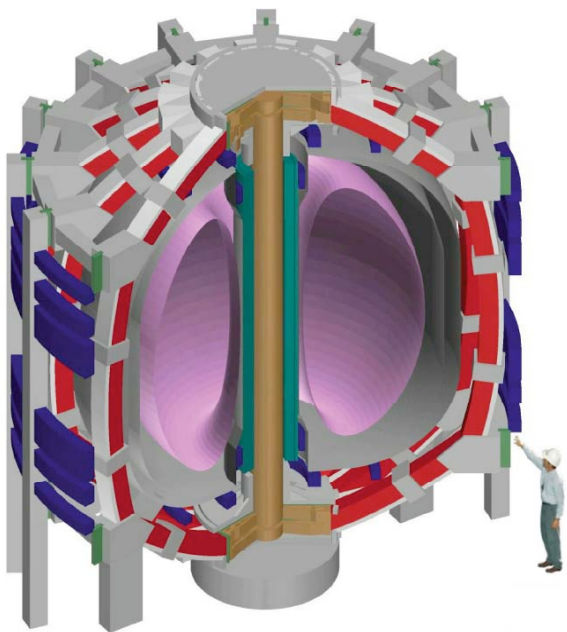


Fig. 21. Isometric Schematic of NSST Device. The NSST at 5 – 10 MA is a performance-extension step to demonstrate the physics viability of ST at fusion parameters.

lower at lower toroidal field of ~ 3.5 kG. This may be due to the generally improving electron confinement with the increasing toroidal field. Clearly, the confinement behavior must be well understood in NSTX to gain sufficient confidence for the required

confinement for $Q \sim 2$ performance in NSST.

6.4. NSST Device Design Overview - A flexible NSST device design is being developed. An isometric view is shown in Fig. 21. The magnets are liquid-nitrogen cooled to allow long pulse as well as high performance operation. To facilitate rapid progress for the NSST research program, an innovative ohmic solenoid can deliver sufficient flux (~ 15 Wb) for 10 MA operation with full swing and 6 MA operation with half swing (~ 8.5 Wb). With inboard PF-1 coils, a strong plasma-shaping capability (elongation $\kappa = 2.7$, triangularity $\delta = 0.6$) is incorporated in the design. The outboard PF coils are placed sufficiently far from the plasma to reduce local shape distortions. The device is designed with a removable center stack to facilitate remote maintenance and to allow for upgrades. The present NSST design utilizes a TFTR-like site with the peak electrical power of 800 MW and energy per pulse of 4.5 GJ and long pulse auxiliary heating and current drive systems (30 MW of NBI and 10 MW of RF). The toroidal cryogenic coil system is estimated to require about 300 MW of electrical power. To explore alpha-physics in high- β plasmas, the existing tritium handling capability can be utilized. The double-walled vacuum vessel is an effective radiation shield such that work restrictions around the machine should be similar to those of TFTR though the total neutron flux would be an order of magnitude larger. About 1000 DT shots are assumed in the estimate. Remote maintenance is however required for the internal components after the initiation of the D-T campaign for NSST. The ST geometry provides a unique opportunity for relatively simple remote maintenance. It is envisioned that the remote maintenance will be performed with the center-stack removed from the device. Once the center-stack is removed, it is relatively straightforward to perform maintenance and repair of the internal vacuum vessel component as well as the center stack. The NSST facility can be built cost effectively by utilizing the existing fusion infrastructure such as power supplies and heating systems.

6.5. NSST TF Design Improvement -The TF joint design in NSST is very challenging due to the high toroidal field and OH solenoid fringing field at the joint region. The previous design called for joints similar to NSTX to make the center-stack completely demountable.⁽⁴⁾ However, the recent studies on NSTX revealed the complex nature of such high current, highly stressed joints in the presence of non-uniform conductor temperature rise due to the non-uniform current distribution. Clearly, if the joints can be eliminated, it is advantageous from fabrication, operational, and maintenance point of view. One possible solution is to use the e-beam welding technique. This weld would move the electrical joint to larger major radius which would greatly reduce the stress at the joint by reducing the toroidal magnetic field value due to the $1/R$ field dependence and lower OH solenoid fringing field values. The larger major radius also offers more space for the joints as well as for the support structures. The OH solenoid and PF 1 coils are then wound around the TF bundle. While this design captures the OH solenoid, since the fabrication cost of the OH solenoid and the PF 1 is only a small fraction of the TF coil joint fabrication cost, this configuration should be cost effective. The new e-beam welded design would also make the one-layer joint design (compared to the previous two-layer design) possible. This would make all the

joints identical which would greatly simplify the design, manufacturing and maintenance.

7. SUMMARIES AND DISCUSSIONS

The NSTX team with its large number of national and international collaborating institutions has steadily enhanced the facility and diagnostic capabilities since the first plasma in 1999. The initial period focused on the basic plasma operating capabilities including the development of real-time plasma control, impurity and surface conditioning techniques, fueling systems, NBI and HHFW heating and current drive systems, and the solenoid-free plasma start-up systems. An extensive set of plasma diagnostics has also been introduced for the magnetic, kinetic profiles, x-rays, energetic particle, boundary physics, and fluctuation measurements. A between-shots EFIT plasma equilibrium reconstruction has successfully incorporated the plasma rotation and recently the MSE data. A recent diagnostic development is the high-k microwave scattering system now being installed to explore electron transport relevant fluctuations including ETGs. Lithium based particle control is being introduced.

Thus far, NSTX has achieved its initial goal of attaining the plasma toroidal beta of $\sim 40\%$ and long pulse high performance discharges with bootstrap current fraction of $\sim 50\%$ with relatively good global plasma confinement time. Ion transport comparable to neo-classical is observed over much of the plasma profiles. Many of the achieved dimensionless plasma parameters are approaching those required for the Component Test Facility. The research focus is now shifting toward accessing the ST power plant relevant advanced regimes of $\sim 40\% \beta_T$ and $\sim 100\%$ non-inductive current drive through strong plasma shaping ($\delta \sim 0.8$, $\kappa \sim 2.6$) and profile control. New PF 1A coils have been installed to achieve this shaping at high elongation, and EF/RWM coils powered by SPA have been installed to enable the plasmas operation at well above the no-wall β limit.

As a next step, the NSST facility is envisioned to provide the necessary physics basis for the design and construction of a compact ST-based CTF, while developing advanced physics scenarios for CTF and attractive DEMO. To support its mission, the NSST facility, with up to 10 MA of plasma current, is designed with advanced physics features. Tritium operation in NSST will enable the alpha-particle and isotope scaling research at high- β for the first time, providing a valuable database for an attractive Demo. The removable center-stack design can facilitate the remote maintenance of the NSST internal hardware. A significant improvement in the center-stack design for NSST has been also described.

Table 1. Major Diagnostic Systems Installed on NSTX

Confinement Studies

Magnetics for equilibrium reconstruction
 Diamagnetic flux measurement
 Multi-pulse Thomson scattering (30 ch, 60 Hz)
 CHERS: $T_i(r)$ and $V_\phi(r)$ (51 ch)
 Neutral particle analyzer (2D scanning)
 FIRETIP interferometer (119 μ m, 6 ch)
 Density Interferometer (1 mm, 1ch)
 Visible bremsstrahlung radiometer (1 ch)
 Midplane tangential bolometer array
 X-ray crystal spectrometer: $T_i(0)$, $T_e(0)$

MSE-CIF (8ch)

MHD/Fluctuation/Waves

High-n and high-frequency Mirnov arrays
 Ultra-soft x-ray arrays – tomography (4)
 Fast X-ray tangential camera (2 μ s)
 Microwave reflectometers
 FIRETIP polarimeter (119 μ m, 6 ch, 600 kHz)
 Tangential microwave scattering
 Electron Bernstein wave radiometer
 Fast lost-ion probe (energy/pitch angle resolving)
 Fast neutron measurement
 Locked-mode detectors
 RWM sensors (n = 1, 2, and 3)

Edge/divertor studies

Reciprocating Langmuir probe
 Gas-puff Imaging (2 μ sec)
 Fixed Langmuire probes (24)
 Edge Rotation Diagnostics (T_i , V_ϕ , V_{pol})
 1-D CCD H_α cameras (divertor, midplane)
 2-D divertor fast visible camera
 Divertor bolometer (4 ch)
 IR cameras (30Hz) (3)
 Tile temperature thermocouple array
 Scarpe-off layer reflectometer
 Edge neutral pressure gauges

Plasma Monitoring

Fast visible camera
 Visible survey spectrometer
 UV survey spectrometer
 VUV transmission grating spectrometer
 Fusion chamber neutron measurement
 Visible filterscopes
 Wall coupon analysis
 X-ray crystal spectrometer (astrophysics)

References

- (1) M. Y-K Peng, D.J. Strickler, Nuclear Fusion **26**, 576 (1986).
- (2) M. Ono, et al., "Exploration of Spherical Torus Physics in the NSTX Device", Nucl. Fusion **40**, 557 (2000).
- (3) S. Kaye, et al., Fusion Technology, **36**, 16 (1999).
- (4) M. Ono, et al., "Next-step spherical torus experiment and spherical torus strategy in the course of development of fusion energy" Nucl. Fusion **44**, 452 (2004).
- (5) J. Menard, et al., "Ideal MHD Stability Limits of Low Aspect Ratio Tokamak Plasmas," Nucl. Fusion **37**, 595 (1997)
- (6) E. Synakowski et al., Nucl Fusion **43**, 1653 (2003).
- (7) C. Neumeyer et al., the IEEE SOFE Conference, 99CH3050 (1999).
- (8) J. Chrzanowski, et al., the IEEE SOFE Conference, 99CH3050 (1999).
- (9) C. Neumeyer et al., "Design and commissioning of the new Toroidal Field Coil for the National Spherical Torus Experiment (NSTX)", in Proceedings of the 23rd Symposium on Fusion Technology (SOFT), Venice, Italy, 20-24 September 2004.
- (10) D. Gates, et. al., "Progress towards steady state on NSTX," Fourth IAEA Technical Meeting on Steady-State Operation of Magnetic Fusion Devices and MHD of Advanced Systems, Institute for Plasma research, Gandhinagar, India (2005). Submitted to Nuclear Fusion
- (11) S. Kaye, et al., "Progress Towards High Performance Plasmas in the National Spherical Torus Experiment (NSTX)," ", the 20th IAEA

- FusionEnergy Conference, Vilamoura, Portugal, 1-6 November 2004, IAEA-CN-116/OV2-3, accepted for publication in Nuclear Fusion (2005).
- (12) J. R. Ferron, M. L. Walker, L. L. Lao, et al., Nucl. Fusion 38 1055 (1998).
- (13) B.P. LeBlanc et al, Rev. Sci. Instrum. **74**, 1659 (2003).
- (14) S. Kubota et al., "Automatic profile reconstruction for millimeter-wave frequency-modulated continuous-wave reflectometry on NSTX," Rev. Sci. Instrum. **74**, 1477 (2003).
- (15) K.C. Lee, et al., "FIR laser Tangential Interferometry/Polarimetry on NSTX", IEEE transaction on plasma science Vol. 32 No.4, 1721 (2004).
- (16) R. E. Bell, et al., "Kinetic Profiles in NSTX Plasmas," in Proceeding of the 28th European Physical Society (EPS) Conference on Controlled Fusion and Plasma Physics, Madeira, Portugal, June 18-22, 2001.
- (17) T. M. Biewer, et al., "Edge rotation and temperature diagnostic on the National Spherical Torus Experiment", Rev. Sci. Instrum. , **75**, 650-654 (2004)
- (18) T. M. Biewer et al., "Edge Ion Heating by Launched High Harmonic Fast Waves in NSTX", Bull. of Am. Phys. Soc., **49**, 324 (2004). Accepted for publication in Physics of Plasmas.
- (19) S. A. Sabbagh, et al., Nuclear Fusion **41**, 1601 (2001).
- (20) M.G. Bell, et al., "Measurements of Plasma Diamagnetism in NSTX", Bull. of Am. Phys. Soc., **46**, 264 (2001).
- (21) S. A. Sabbagh, et al., "Wall Stabilized Operation in High Beta NSTX Plasmas", the 20th IAEA FusionEnergy Conference, Vilamoura, Portugal, 1-6 November 2004, IAEA-CN-116/EX/3-2.
- (22) A. H. Glasser and M. C. Chance, Bull. Am. Phys. Soc. **42**, 1848 (1997).
- (23) F. Levinton et al., Phys. Rev. Letters **63**, 2060 (1989).
- (24) F. Levinton et al., "Initial Results from the Motional Start Effect Diagnostic on NSTX," Bull. of Am. Phys. Soc., **49**, 221 (2004).
- (25) E. L. Foley and F. M. Levinton, Rev. Sci. Instrum. **75**, 3462(2004).
- (26) Z. Wang and G. A. Wurden, 'Hypervelocity dust beam injection for national spherical torus experiment,' Rev. Sci. Instrum. **75**, 3436 (2004).
- (27) D. Stutman, et al., "Ultrasoft x-ray imaging system for the National Spherical Torus Experiment," Rev. Sci. Instrum. **70**, 572 (1999).
- (28) B. C. Stratton, et al., "Fast X-ray Camera," Rev. Sci. Instrum., vol. 75, p. 3959 (2004).
- (29) S. Kubota, et al., "Reflectometry Measurements of the Electron Density Profile and Fluctuations in NSTX", Bull. of Am. Phys. Soc., **49**, 262 (2004).
- (30) K.C. Lee, et al., "Edge density fluctuation characterization in H-mode and polarimetry measurement via the FIRETIP system on NSTX" Rev. Sci. Instrum. **75** (2004)3433
- (31) D.R. Smith et al. "Status of High-k Scattering System on NSTX", Bull. of Am. Phys. Soc., **49**, 301 (2004).
- (32) E. Mazzucato, T. Munsat, and H. Park, et al., "Fluctuation measurements in tokamak with microwave imaging reflectometry," Physics of Plasmas **9**, 1955 (2002).
- (33) H. Park et al, "Recent advancements in microwave imaging plasma diagnostics," Rev. Sci. Instrum., **74**, 4239 (2003).
- (34) S. S. Medley and A. L. Roquemore, "Neutral Particle Analyzer Diagnostic on the National Spherical Torus Experiment," Rev. Sci. Instrum. **75**, 3625 (2004)
- (35) D. Darrow, "Pitch angle resolved measurements of neutral beam ion loss from NSTX," Bull. of Am. Phys. Soc., **49**, 301 (2004).
- (36) W.W. Heidbrink, et al., "The Confinement of Dilute Populations of Beam Ions in the National Spherical Torus Experiment," Nucl. Fusion **43**, 883 (2003).
- (37) S. S. Medley, et al., "MHD-induced Energetic Ion Loss during H-mode Discharges in the National Spherical Torus Experiment," Nucl. Fusion **44**, 1158 (2004).
- (38) E.D. Fredrickson, et al, "Wave driven fast ion loss in the National Spherical Torus Experiment," Phys. of Plasmas **10** (2003) 2852
- (39) E. D. Fredrickson, et al., "Phenomenology of compressional Alfvén eigenmodes," Phys. of Plasmas **11** (2004) 3653.
- (40) J. Boedo, et al., to be published in Rev. Sci. Instrum. (scheduled April 2005).
- (41) S.J. Zweben, R.J. Maqueda, D.P. Stotler et al., "High Speed Imaging of Edge Turbulence in NSTX," Nuclear Fusion **44**, 134 (2004).
- (42) N. Nishino, et. al. "First Results with the NSTX Fast Divertor Camera", Journal of Plasma and Fusion Research **78**, 1278 (2002).
- (43) R. Maingi, et al., "Observation of a high performance operating regime with small edge localized modes in the National Spherical Torus Experiment," Nuclear Fusion **45**, 264 (2005).
- (44) A. Bader, C. H. Skinner, et al., "Development of an Electrostatic Dust Detector for Use in a Tokamak Reactor," Rev. Sci. Instrum. **75**, 370 (2004).
- (45) H.W. Kugel, et. al., "NSTX High Field Side Gas Fueling System," in Proceedings of the 20th IEEE/NPSS Symposium on Fusion Engineering, Oct. 14-17, 2003, San Diego CA.
- (46) R. Maingi, et. al., "Effect of gas fuelling location on H-mode access in NSTX," Plasma Phys. Control Fusion **46**, A305 (2004).
- (47) V. A. Soukhanovskii, et al., "Supersonic gas injector for fueling and diagnostic applications on the National Spherical Torus Experiment," Rev. of Sci. Instrum. **75**, (2004) 4320.
- (48) R. Raman, "Fueling requirements for advanced tokamak operation," Currents trends in international fusion research: A Review, 7-11 March 2005, Washington, DC.
- (49) H. W. Kugel, et al., "Development of NSTX Particle Control Techniques," Proceedings of the 16th Int. Conf. on Plasma Surface Interaction in Controlled Fusion Devices, May 24-28, 2004, Portland, Maine (accepted for publication in J. Nucl. Mater.)
- (50) R. Majeski, et al., "Testing of liquid lithium limiters in CDX-U," Fusion Engineering and Design **72**, 121(2004).
- (51) H.W. Kugel, et al., "Initial NSTX Lithium Pellet Injection" Bull. Am. Phys. **49**, 221(2004).
- (52) T. Stevenson, et al., "A Neutral Beam Injector Upgrade for NSTX ", Princeton Plasma Physics Laboratory Report number 3651, (2002).
- (53) M. Ono, "High harmonic fast waves in high beta plasmas," Phys. of Plasmas **2**, 4075 (1995).
- (54) P. Ryan et al, in Fusion Energy 2002 (Proc. 19th Int. Conf. Lyon, 2002) (Vienna: IAEA) CD-ROM file EX/P2-13.
- (55) J. W. Wilson et al., "High Harmonic Fast Wave Heating on NSTX," Bull. Am. Phys. **49**, 69 (2004).
- (56) R. Raman et al., "Non inductive solenoid free plasma startup using coaxial helicity injection," accepted for publication as a Letter in

-
- Nuclear Fusion (2005).
- (57) Y. Takase, et al., "Development of a Completely CS-less Tokamak operation in JT-60U," in Fusion Energy 2004 (Proc. 20th Int. Conf. Vilamoura, 2004, EX/P4-34).
- (58) Y. Ono and M. Inomoto, "Ultra-High Beta Spherical Tokamak Formation by Use of Oblate Field-Reversed Configuration", Physics of Plasmas, **7**, 1863 (2000).
- (59) A. Sykes, et al., "Plasma formation without a central solenoid in a Spherical Tokamak", Bull. Am. Phys. **49**, 68 (2004).
- (60) W. Choe, et al., "Solenoid-Free Toroidal Plasma Start-Up Concept Utilizing Only the Outer Poloidal Field Coils and a Conducting Center-post," in Fusion Energy 2004 (Proc. 20th Int. Conf. Vilamoura, 2004, IC/P6-35).
- (61) S. Sabbagh, et al., Nuclear Fusion **41**, 1601 (2001).
- (62) S. Sabbagh, et al., Phys. Plasmas **9**, 2085 (2002).
- (63) J. Menard, et al., " β -Limiting MHD instabilities in improved-performance NSTX spherical torus plasmas," Nucl. Fusion **43** 330 (2003).
- (64) A.M. Garofalo, et al., "Sustained rotational stabilization of DIII-D plasmas above the no-wall beta limit," Phys. of Plasmas **9**, 1997, (2002).
- (65) A.C. Sontag, S.A. Sabbagh, W. Zhu, et al "Resistive Wall Mode Stabilization of High Beta Plasmas in the National Spherical Torus Experiment," to be published in Phys. Plasmas (2005).
- (66) C. E. Kessel, et al., "Advanced ST Plasma Scenario Simulations for NSTX," in Fusion Energy 2004 (Proc. 20th Int. Conf. Vilamoura, 2004, EX/P4-34). Submitted for publication in Nuclear Fusion.
- (67) G. Taylor, *et al.*, "Efficient generation of non-inductive, off-axis, Ohkawa current, driven by electron Bernstein waves in high b , spherical torus plasmas. Phys. of Plasmas **11**, 4733 (2004)
- (68) G. Taylor, *et al.*, "Efficient coupling of thermal electron Bernstein waves to the ordinalry electromagnetic mode on the National Spherical Torus Experiment (NSTX), Phys. of Plasmas **12**, 052511 (2005).

External Distribution

Plasma Research Laboratory, Australian National University, Australia
Professor I.R. Jones, Flinders University, Australia
Professor João Canalle, Instituto de Fisica DEQ/IF - UERJ, Brazil
Mr. Gerson O. Ludwig, Instituto Nacional de Pesquisas, Brazil
Dr. P.H. Sakanaka, Instituto Fisica, Brazil
The Librarian, Culham Science Center, England
Mrs. S.A. Hutchinson, JET Library, England
Professor M.N. Bussac, Ecole Polytechnique, France
Librarian, Max-Planck-Institut für Plasmaphysik, Germany
Jolan Moldvai, Reports Library, Hungarian Academy of Sciences, Central Research
Institute for Physics, Hungary
Dr. P. Kaw, Institute for Plasma Research, India
Ms. P.J. Pathak, Librarian, Institute for Plasma Research, India
Dr. Pandji Triadyaksa, Fakultas MIPA Universitas Diponegoro, Indonesia
Professor Sami Cuperman, Plasma Physics Group, Tel Aviv University, Israel
Ms. Clelia De Palo, Associazione EURATOM-ENEA, Italy
Dr. G. Grosso, Istituto di Fisica del Plasma, Italy
Librarian, Naka Fusion Research Establishment, JAERI, Japan
Library, Laboratory for Complex Energy Processes, Institute for Advanced Study,
Kyoto University, Japan
Research Information Center, National Institute for Fusion Science, Japan
Professor Toshitaka Idehara, Director, Research Center for Development of Far-Infrared Region,
Fukui University, Japan
Dr. O. Mitarai, Kyushu Tokai University, Japan
Mr. Adefila Olumide, Ilorin, Kwara State, Nigeria
Dr. Jiangang Li, Institute of Plasma Physics, Chinese Academy of Sciences, People's Republic of China
Professor Yuping Huo, School of Physical Science and Technology, People's Republic of China
Library, Academia Sinica, Institute of Plasma Physics, People's Republic of China
Librarian, Institute of Physics, Chinese Academy of Sciences, People's Republic of China
Dr. S. Mirnov, TRINITI, Troitsk, Russian Federation, Russia
Dr. V.S. Strelkov, Kurchatov Institute, Russian Federation, Russia
Kazi Firoz, UPJS, Kosice, Slovakia
Professor Peter Lukac, Katedra Fyziky Plazmy MFF UK, Mlynska dolina F-2, Komenskeho Univerzita,
SK-842 15 Bratislava, Slovakia
Dr. G.S. Lee, Korea Basic Science Institute, South Korea
Dr. Rasulkhozha S. Sharafiddinov, Theoretical Physics Division, Institute of Nuclear Physics, Uzbekistan
Institute for Plasma Research, University of Maryland, USA
Librarian, Fusion Energy Division, Oak Ridge National Laboratory, USA
Librarian, Institute of Fusion Studies, University of Texas, USA
Librarian, Magnetic Fusion Program, Lawrence Livermore National Laboratory, USA
Library, General Atomics, USA
Plasma Physics Group, Fusion Energy Research Program, University of California at San Diego, USA
Plasma Physics Library, Columbia University, USA
Alkesh Punjabi, Center for Fusion Research and Training, Hampton University, USA
Dr. W.M. Stacey, Fusion Research Center, Georgia Institute of Technology, USA
Director, Research Division, OFES, Washington, D.C. 20585-1290

The Princeton Plasma Physics Laboratory is operated
by Princeton University under contract
with the U.S. Department of Energy.

Information Services
Princeton Plasma Physics Laboratory
P.O. Box 451
Princeton, NJ 08543

Phone: 609-243-2750
Fax: 609-243-2751
e-mail: pppl_info@pppl.gov
Internet Address: <http://www.pppl.gov>